and increased permeability precedes deposition of immune complexes in the glomerular capillary wall. *Am J Pathol* 105: 114–120, 1981.
62. Fishman RM, Moore GL, Zegna A, Marini MA: High-performance liquid chromatographic evaluation of pyridoxal 5'-phosphate hemoglobin derivatives produced by different reduction procedures. *J Chromatogr* 532: 55–64, 1990.
63. Flamenbaum W, Gehr M, Gross M, Kaufman J, Hamburger R: Acute renal failure associated with myoglobinuria and hemoglobinuria, in Brenner BM, Lazarus JM (eds), *Acute Renal Failure*, Philadelphia, Saunders, 1983, pp. 269–282.
64. Pimstone NR: Renal degradation of hemoglobin. *Semin Hematol* 9: 31–42, 1972.
65. Tenhunen R, Marver HS, Schmid R: Microsomal heme oxygenase. Characterization of the enzyme. *J Biol Chem* 244: 6388–6394, 1969.
66. Tenhunen R, Marver HS, Schmid R: The enzymatic catabolism of hemoglobin: stimulation of microsomal heme oxygenase by hemin. *J Lab Clin Med* 75: 410–421, 1970.
67. Kutty RK, Daniel RF, Ryan DE, Levin W, Maines MD: Rat liver cytochrome P-450b, P-450b, and P-420c are degraded to biliverdin by heme oxygenase. *Arch Biochem Biophys* 260: 638–644, 1988.
68. Lahdevirta J, Tenhunen R: Heme catabolism in human kidneys, effect of various nephritides. *Clin Chim Acta* 77: 125–130, 1977.
69. Feola M, Simoni J, Tran R, Canizaro PC: Nephrotoxicity of hemoglobin solutions. *Biomater Artif Cells Artif Organs* 18: 233–249, 1990.
70. Ning J, Peterson LM, Anderson PJ, Biro GP: Systemic hemodynamic and renal effects of unmodified human SFHS in dogs. *Biomater Artif Cells Immobil Biotechnol* 20: 723–727, 1992.
71. Rose BD Black RM: *Manual of Clinical Problems in Nephrology*, Boston, Little, Brown, 1988, pp. 3–244.
72. Noto A, Ogawa Y, Mori S, *et al.*: Simple, rapid spectrophotometry of urinary A-acetyl-β-D-glucosaminidase, with use of a new chromogenic substrate. *Clin Chem* 29: 1713–1716, 1983.
73. Paller MS, Hoidal JR, Ferris TF: Oxygen free radicals in ischemic acute renal failure in the rat. *J Clin Invest* 74: 1156–1164, 1984.
74. Simoni J, Simoni G, Lox CD, Feola M: Reaction of human endothelial cells to bovine hemoglobin solutions and tumor necrosis factor. *Artif Cells Blood Substit Immobil Biotechnol* 22: 777–787, 1994.
75. Yoshida Y, Kashiba K, Niki E: Free radical mediated oxidation of lipid induced by hemoglobin in aqueous dispersions. *Biochim Biophys Acta* 1201: 165–172, 1994.
76. Simoni J, Simoni G, Lox CD, *et al.*: Evidence for the direct inhibition of endothelin-1 secretion by hemoglobin in human endothelial cells. *ASAIO J* 41: M641–651, 1995.
77. Simoni J, Simoni G, Lox CD, *et al.*: Cytokines and PAF release from human monocytes and macrophages: effect of hemoglobin and contaminants. *Artif Cells Blood Substit Immobil Biotechnol* 22: 525–534, 1994.
78. Simoni J, Simoni G, Lox CD, *et al.*: Modified Hb solution with desired pharmacological properties, does not activate the transcription factor NF-kappa B in human vascular endothelial cells. *Artif Cells Blood Substit Immobil Biotechnol* 25: 193–210, 1997.
79. Simoni J, Simoni G, Lox CD, *et al.*: Expression of adhesion molecules and von Willebrand factor in human coronary artery endothelial cells incubated with differently modified hemoglobin solutions. *Artif Cells Blood Substit Immobil Biotechnol* 25: 211–225, 1997.
80. Dalay JW, Kuroda Y, Phillis JW, Shimazu H, Ui M: *Physiology and Pharmacology of Adenosine Derivatives*, New York, Raven Press, 1983, pp. 1–299.
81. Haynes J Jr, Obiako B, Thompson WJ, Downey J: Adenosine induced vasodilation: receptor characterization in pulmonary circulation. *Am J Physiol* 268: H1862–1868, 1995.
82. Yamagishi T, Yaangisawa T, Satoh K, *et al.*: Relaxant mechanism of cyclic AMP-increasing agents in porcine coronary artery. *Eur J Pharmacol* 251: 253–262, 1994.
83. Matsunaga T, Okumura K, Tsunoda R, *et al.*: Role of adenosine in regulation of coronary flow in dogs with inhibited synthesis of endothelium-derived nitric oxide. *Am J Physiol* 270: H427–434, 1996.
84. Maggirwar SB, Dhanraj DN, Somani SM, Ramkumar V: Adenosine acts as an endogenous activator of the cellular antioxidant defense system. *Biochem Biophys Res Commun* 201: 508–515, 1994.
85. Bouma MG, Van Der Wildenberg Fajm, Buurman WA: Adenosine inhibits cytokine release and expression of adhesion molecules by activated human endothelial cells. *Am J Physiol* 270: C522–C529, 1996.
86. Cronstein BN: Adenosine, and endogenous anti-inflammatory agent. *J Appl Physiol* 76: 5–13, 1994.

Development of a Low Flow Resistance Intravenous Oxygenator

WILLIAM J. FEDERSPIEL, MARIAH S. HOUT, TODD J. HEWITT, LAURA W. LUND, SHELLY A. HEINRICH, PHILIP LITWAK, FRANK R. WALTERS, GARY D. REEDER, HARVEY S. BOROVETZ, AND BRACK G. HATTLER

A potentially attractive support device for patients with acute respiratory failure is an intravenous membrane oxygenator. One problem, however, is that the membrane surface area required for sufficient gas exchange can unduly increase vena caval pressure drop and impede venous return. The purpose of this study was to design and develop an intravenous oxygenator that would offer minimal venous flow resistance *in situ*. The device uses a constrained fiber bundle of smaller cross sectional size than the vena cava so as to effect an intentional shunt flow of venous blood around the fiber bundle and reduce the venous pressure drop caused by the device. A pulsating balloon within the fiber bundle redirects part of this shunt flow into reciprocating flow in and out of the fiber bundle. This offers dual advantages: 1) Blood flow through the fiber bundle is mainly perpendicular to the fibers; and 2) the requisite energy for driving flow comes largely

From the Artificial Lung Laboratory, McGowan Center for Artificial Organ Development, Department of Surgery, Department of Chemical Engineering, and Bioengineering Program, University of Pittsburgh, Pittsburgh, Pennsylvania.

Reprint requests: William J. Federspiel, PhD, Artificial Lung Laboratory, University of Pittsburgh, Rm. 428, Biotechnology Center, 300 Technology Dr., Pittsburgh, PA 15219.

from the pneumatic system pulsating the balloon, not from a venous pressure drop. In this mode a full length device with a 2 cm fiber bundle in a 2.5 cm blood vessel would offer a pressure drop of only a few millimeters of mercury. The use of constrained fiber bundles requires good uniformity of fiber spacing for effective gas exchange. Several prototypes have been fabricated, and CO_2 and O_2 exchange rates of up to 402 and 347 ml/min/m^2 have been achieved during acute animal implantation. *ASAIO Journal* 1997; 43: M725–M730.

Acute respiratory distress syndrome (ARDS) remains a major cause of morbidity and mortality for severely ill patients.[1] ARDS is characterized by a rapid and progressive malfunction of the lung due to increased pulmonary endothelial and epithelial permeability, leading to fluid accumulation in interstitial and alveolar spaces of the lung.[2] The National Institutes of Health indicates that 150,000 cases of ARDS occur each year, and the fatality rate is ~50% despite current methods of supportive strategy, including assisted respiration by mechanical ventilation and extracorporeal membrane oxygenation. A potentially attractive alternative to assisted respiration in ARDS patients is intravenous oxygenation, in which a bundle of hollow fiber membranes (manifolded to gas supply and removal lines) is placed within the vena cava system to supply oxygen and remove carbon dioxide before blood reaches the failing lung. The only intravenous oxygenator used clinically (in Phase I trials) was the IVOX device,[3] which accomplished gas exchange rates up to 30% of metabolic requirements in ARDS patients.[4] The IVOX devices were implanted for up to 29 days, showed little degradation in gas exchange, and did not result in serious thromboembolic complications. Nevertheless, the IVOX clinical studies suggested that higher levels of gas exchange would be needed for clinically effective intravenous oxygenation.

A direct means of increasing gas exchange in intravenous oxygenators is to increase fiber membrane surface area, by using either more and/or smaller hollow fibers. Moreover, effective gas exchange requires that the hollow fibers be well distributed within the cross section of the vena cava, maximizing exposure to all blood elements flowing back to the heart. The crimping of hollow fibers in the IVOX device[3] helped distribute the fibers uniformly within the vena cava cross section and improved gas exchange. Through analogous mechanisms to those that increase gas transfer, maximizing blood contact with fibers also increases momentum transfer and hence fiber drag on blood flow. One problem is that increasing fiber membrane area to achieve adequate gas exchange increases blood flow resistance past the oxygenator, leading to a potentially large vena caval pressure drop and impeding venous return. The purpose of this study was to design, develop, and test an intravenous oxygenator that would offer minimal venous flow resistance *in situ*.

Design Concept for Low Flow Resistance Intravenous Oxygenator

The concept for a low flow resistance intravenous oxygenator arose from development of the University of Pittsburgh Intravenous Membrane Oxygenator (IMO).[5,6] The IMO device uniquely employs a pulsating balloon located concentrically within the fiber bundle to create additional fluid convection and mixing within the vena cava subjacent to the fibers. Previous IMO designs for implantable prototypes[6] used free fibers, which were fibers plotted into manifolds at each end of the device but that were otherwise free to move relative to one another. Pulsations of the balloon moved fibers around within the available vessel cross section between balloon and vessel wall, which helped increase blood-fiber interactions. In contrast, the low flow resistance version of the IMO uses a constrained fiber bundle, where fibers are woven as a fabric (or mat) around the balloon with sufficient constraint so as not to move significantly with balloon pulsation.

The principle underlying reducing blood flow resistance with a constrained fiber bundle is illustrated in **Figure 1**, in both cross sectional and longitudinal views. The key element is a fiber bundle of smaller cross sectional than vessel size (**Figure 1A**), i.e., $D_{\text{fiber bundle}} < D_{\text{vessel}}$. This creates an intentional shunt flow Q_L of venous blood around the fiber bundle (**Figure 1B**), which reduces the blood flow resistance associated with the device. Fiber bundle size can be selected to target some minimal acceptable pressure drop. The intentional shunt flow of blood around the fiber bundle would significantly degrade gas exchange if not for the pulsations of the balloon. The convective flow $Q_b(t)$ driven by balloon pulsations directs the shunt flow perpendicularly across the longitudinally arranged fiber bundle, directly increasing gas transfer. This strategy thus exploits the superior mass transfer associated with cross flow as compared with parallel flow. Moreover, the principal energy required to drive blood flow through the fiber bundle comes from the balloon drive system, not from a pressure drop imposed on venous return to the heart.

Design Computations for Pressure Drop

The required fiber bundle size to achieve a low pressure drop was estimated using a simplified model of the device in a vessel of human vena caval dimensions. The overall diameter of the IMO ($D_{\text{fiber bundle}}$ in **Figure 1**) must be small enough to engender a pressure drop across the device of only a few millimeters of mercury, while maintaining specified gas exchange rates. Since venous return moves through the annular shunt volume around the device, the pressure drop can be estimated for design purposes using equations for flow through an annulus[7] with an outside diameter of D_{vessel}, an inside diameter of $D_{\text{fiber bundle}}$, and a flow rate of Q_L. This calculation treats the IMO as a solid cylinder with a diameter of $D_{\text{fiber bundle}}$. The purpose of this model is specifically to isolate and examine the sensitivity of the pressure drop to the bundle diameter. Accordingly, the model ignores the effects of space between the fibers available for flow that would tend to diminish pressure drop as well as the effects of the dynamic interaction between the balloon generated flow and the steady-state venous flow (Q_L) that would tend to augment pressure drop. In simplified modifications to the model, these effects were found to be minimal with respect to the effect on pressure drop of the bundle diameter relative to the vena caval diameter.

Figure 2 shows the predicted pressure drop across the IMO as a function of the device diameter ($D_{\text{fiber bundle}}$) in a fluid with similar viscosity to blood (3 cps) at a flow rate of 3 L/min. The vessel diameter is assumed to be 2.5 cm in both cases, and pressure drops are computed for 20 and 40 cm length devices, respectively. The pressure drop is very small when the IMO

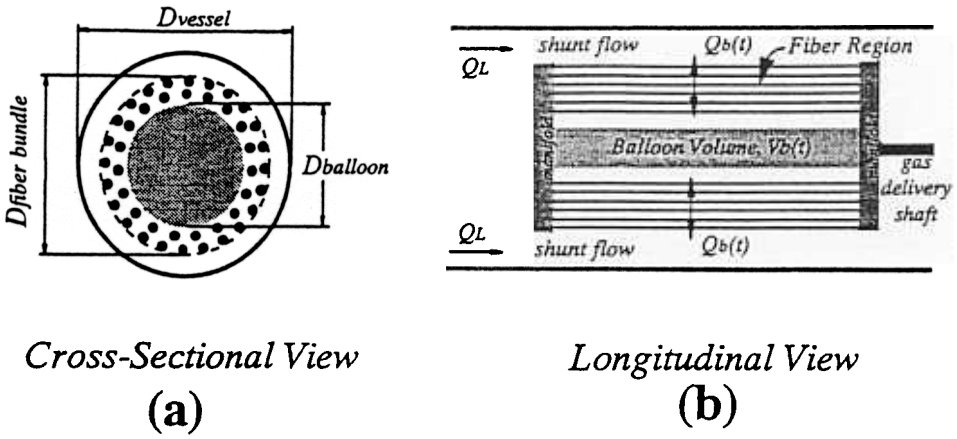

Figure 1. Design concept for a low flow resistance intravenous membrane oxygenator.

diameter is small and approaches infinity as $D_{\text{fiber bundle}}$ approaches D_{vessel}. At ~2.0 cm, or 80% of vessel wall diameter, the pressure drop curve steepens so that for small increases in bundle size, there are more significant increases in pressure drop. To avoid this segment of the curve, the design range for minimal pressure drop and maximal gas exchange was chosen to be between 1.5 and 2.0 cm. This model also predicts that the pressure drop across a 40 cm IMO will not be twice that across a 20 cm device. For instance, the pressure drop for a 20 cm length, 2.15 cm diameter IMO is 5.5 mmHg, while that for a 40 cm device with the same diameter is 10 mmHg. This difference is due to entrance effects as the flow becomes fully developed and is less important in longer devices and at larger fiber bundle diameters.

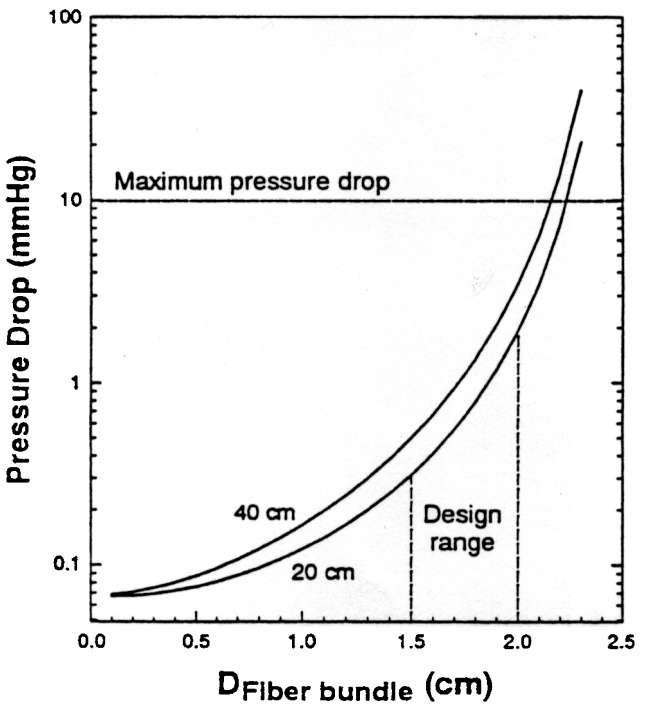

Figure 2. Calculated pressure drop across the intravenous membrane oxygenator *vs* fiber bundle diameter. Calculations are based on a fluid with viscosity comparable to blood (3.0 cps) at a flow rate of 3 L/min.

Materials and Methods

Two prototype designs for low resistance intravenous oxygenators were fabricated for *in vitro* and *in vivo* testing. **Table 1** summarizes the pertinent characteristics of both devices. Both fibers were constructed with constrained microporous fiber bundles, arranged longitudinally to the axis of the device, around the balloon. The first device, D14, uses a larger diameter KPF 280 fiber (Mitsubishi Rayon America Co., New York, NY) that results in a device with a lesser overall fiber surface area than that of the second device, D17, which uses a smaller diameter Celgard 240 fabric (Hoechst Celanese, NC). Aside from the slight differences in fiber diameter and surface area, the device configurations were identical.

The pressure drop and gas exchange performance of the D14 and D17 constrained fiber prototypes were characterized in our *in vitro* (mock vena cava) test loop, which has been described in detail previously[6] along with associated procedures and analyses. The test loop consists of a 1 in diameter compliant tube in which devices are placed and perfused with distilled water at flow rates from 1 to 5 L/min at physiologic temperature (37°C). Pressure ports are positioned immediately before and after the device location. The mean pressure drop across the device is then determined from the difference in manometer column heights. Oxygen sweep gas flows through the fiber lumina at 3 L/min, and the water side PO_2 is measured

Table 1. Intravenous Oxygenator Specifications

	IMO D14	IMO D17
Fiber type	KPF 280 mat	Celgard 240 fabric
Number of fibers	385	665
Fiber OD/ID (μm)	380/280	300/240
Bundle diameter (cm)	~1.6	~1.7
Bundle length (cm)	18	20
Surface area (m^2)	0.085	0.128

OD, outside diameter; ID, inside diameter.

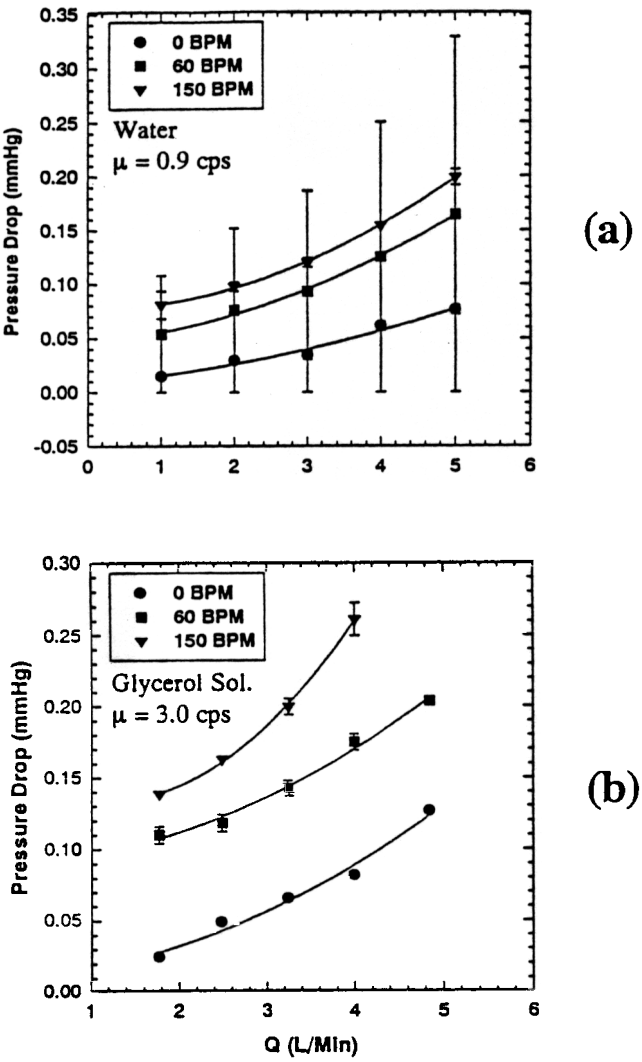

Figure 3. Mean pressure drops with varying flow and balloon pulsation in distilled water (a) and 40% glycerol solution (b).

before and after the device to determine the O_2 exchange rate. A deoxygenator used within the test loop maintains "venous" PO_2 (i.e., pre-device PO_2) at a steady state value. The pressure drop and gas exchange are measured at each flow rate over a range of balloon pulsation rates up to 150 beats/min. Pressure drops were also measured following the same protocol but using a 40% glycerol solution in the test circuit, which has a viscosity of 3 cps and thus better approximates the pressure drop in blood.

The D14 oxygenator prototype was tested *in vivo* by acute implantation in calves. Surgical implantation of the devices and the medical care of the calves followed the protocol established during *in vivo* testing of the free fiber devices.[8] After implantation, oxygen was pulled through the fiber bundle under vacuum. The central polyurethane balloon was pulsed at several different frequencies using an intra-aortic balloon pump console. At each frequency, the sweep gas flow rate and the fractions of O_2 and CO_2 in the exhaust gas were recorded. These data were used to calculate the magnitude of O_2 delivery and CO_2 removal.[8]

Pressure Drop and Gas Exchange in Bench Tests

Mean Pressure Drops

The pressure drops measured in the *in vitro* test loop increased with flow rate from 0 to 5 L/min and with balloon pulsation frequency from 0 to 150 beats/min, as illustrated in **Figure 3**. The highest mean pressure drop in water at 5 L/min and 150 beats/min was <0.20 mmHg and in the 40% glycerol solution reached only 0.26 mmHg at 4 L/min and 150 beats/min. Under comparable flow rate and pulsation conditions, the pressure drop of the device in the glycerol solution was no more than 1.7 times that in water, significantly less than the more than three fold difference in the respective viscosities. This indicates that the pressure drop is partially related to inertial or density related losses and not entirely to viscosity effects, implying that any differences in the viscosity of the glycerol solution compared with non Newtonian blood viscosity will be mitigated.

The cross sectional diameter of both devices tested was ~1.7 cm. In **Figure 2**, the predicted pressure drops using the design model for a device 20 cm in length and 1.7 cm in diameter are ~0.5 mmHg in a fluid with a viscosity of 3 cps, while those measured *in vitro* in the glycerol solution without balloon pulsation are only 0.07 mmHg. That the predicted pressure drops significantly exceed those measured experimentally may be due to the axial positioning of the device *in vitro*. While the model calculations assume concentricity of vessel and fiber bundle, in practice buoyancy forces keep the fiber bundle maximally off center within the cross section of the vessel.

Gas Exchange Performance

The oxygen exchange rates of constrained fiber prototypes in water flowing at 3 L/min, normalized to respective device membrane area, are displayed in **Figure 4** as functions of the balloon pulsation rate in beats per minute. The constrained fiber prototypes had fiber bundles fabricated from either the Mitsubishi KPF 280 mat (D14.2) or the Celgard 240 fabric array (D17.1). Shown for comparison is the gas exchange rate of a previous prototype fabricated with a free fiber bundle

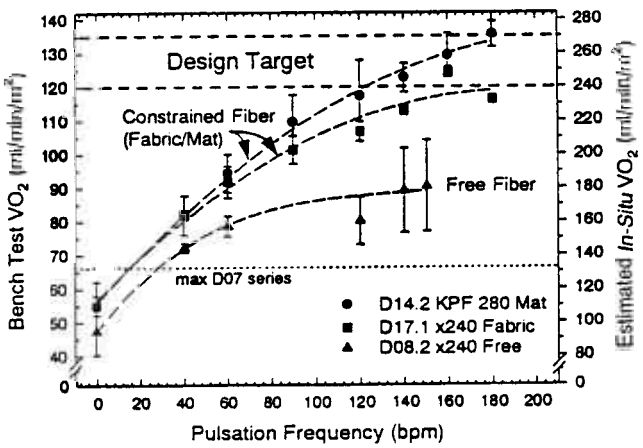

Figure 4. Oxygen exchange rate in water of intravenous membrane oxygenator prototypes as a function of balloon pulsation frequency at a flow rate of 3 L/min.

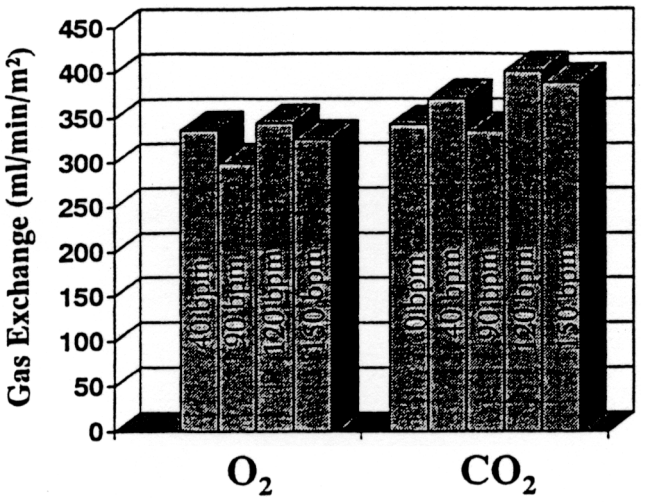

Figure 5. *In vivo* gas exchange performance of the D14 constrained fiber bundle device.

(D08.2). Whereas the free fiber device exhibited a plateau of gas exchange rate with increasing balloon pulsation rate,[6] the rate of gas exchange in the constrained fiber prototypes continually increased as pulsation rate increased. This difference can be specifically attributed to the constrained fiber bundles because the prototypes are otherwise identical and have comparable balloon pulsation dynamics as determined in independent tests. The constrained fiber bundles improve gas exchange by maintaining a more uniform fiber distribution around the pulsating balloon and by reducing fiber motion so as to increase the relative fluid velocity of pulsation flow past the fibers.

The levels of gas exchange accomplished with the constrained fiber bundle devices are within or close to our design target for gas exchange, indicated within the pair of upper dashed lines in **Figure 4**. The design target range is determined as follows: We previously reported use of a data analysis technique whereby gas exchange levels in blood can be estimated from testing results in water[6,9] and that typically a 2 to 2.5 fold greater rate of gas exchange occurs with an IMO device in blood under otherwise comparable conditions. Assuming a conservative factor of 2, the right-hand ordinate displays estimated *in situ* blood exchange values for the devices tested. Our gas exchange design target of 50% of baseline metabolic rates (or ~120–135 ml/min) translates to a normalized target rate of 240–270 ml/min/m^2, assuming an ultimate device with up to 0.5 m^2 of membrane area.

Acute In Vivo Gas Exchange

The *in vivo* gas exchange performance of the D14 device is shown in **Figure 5**. The device achieved a maximum O_2 delivery rate of 336 ml/min/m^2 and a CO_2 removal rate of 402 ml/min/m^2. Of greatest interest is the apparent independence of gas exchange on the rate of balloon pulsation *in vivo* compared with the large effect of balloon pulsation demonstrated *in vitro*. *In vitro* balloon pulsation increases the oxygen delivery by 250%. One possibility is that the mean flow velocity *in vivo*, i.e., the flow rate divided by cross sectional area, is much higher than that encountered *in vitro*. During *in vitro* testing, water is pumped through a test section of 1 in inner diameter at a flow rate of 3 L/min to approximate projected conditions in a human patient. In a calf, however, typical cardiac outputs are 7–10 L/min, suggesting that the flow rate in the inferior vena cava, where the device is positioned for the *in vivo* testing protocol, is ~4.5–6.5 L/min. Also contributing to the high mean blood velocity is the small diameter of the vena cava. By opening the chest cavity of the calf with the device implanted, the diameter of the vena cava was found to be ~¾ in. The pressure drop across the length of the device was found to be 9–16 mmHg *in vivo*, while *in vitro* measurements showed a <1 mmHg pressure drop in a 1 in test section. These results add to the evidence that the inner diameter of the vena cava was <1 in.

The high blood flow rate and small vessel diameter in the calf implantations cause a much higher mean flow velocity past the IMO device than the level used *in vitro*. This would result in an increased baseline gas exchange rate, even in the absence of balloon pulsations. Accordingly, the transverse velocity component imparted by the balloon may contribute very little to the total gas exchange when compared with the contribution of the significant longitudinal component, and gas exchange would appear to be independent of the rate of balloon pulsation. This hypothesis derives further support from considerations of gas exchange levels. It has been shown that under a given set of test conditions, the O_2 exchange rate in blood will equal 2.5 to 3 times that in water.[6] The rate of O_2 exchange achieved by the D14 prototype *in vivo* was over five times the rate of O_2 exchange achieved *in vitro* without balloon pulsation, most likely due to the much higher mean flow velocity *in vivo* compared with that *in vitro*.

We are currently testing this theory by conducting an *in vitro* experiment using a test section with a ¾ in inner diameter. The flow rates used will be in the range of the cardiac outputs measured *in vivo* in calves. If the balloon has little effect under these conditions, future animal experiments may be better performed using an *ex vivo* shunt under test conditions expected in human implants.

Summary

The purpose of this study was to develop an intravenous oxygenator design that minimizes pressure drops across the device in the vena cava, while maintaining oxygen and carbon dioxide exchange rates at required levels. Key aspects of the resulting design include the use of an elongated pulsating balloon positioned concentrically within a constrained bundle of fibers having an overall diameter smaller than that of the vena cava. Theoretical analyses and *in vitro* testing of this device both demonstrate very low pressure drops (<1 mmHg) can be achieved while maintaining sufficient gas exchange. The smaller diameter of the device relative to vena caval diameter allows for a reduced pressure drop across the device, while the pulsation of the balloon provides the energy necessary to drive blood flow perpendicularly into and out of the fiber bank for effective gas exchange. *In vivo* testing of the device, however, was inconsistent with predictions based on the bench test results. Because of variabilities in the animal vena caval geometry and hemodynamics, further bench testing is being conducted to explore the cause of these inconsistencies. An

ex vivo extracorporeal test protocol is also being developed to provide an *in situ* test environment that may more closely approximate the performance of the device in a human patient.

References

1. Matthay MA: The acute respiratory distress syndrome. *N Engl J Med* 334: 1469–1470, 1996.
2. Weinberger SE: *Principles of Pulmonary Medicine.* Philadelphia, Saunders, 1992.
3. Mortensen JD: Intravascular oxygenator: a new alternative method for augmenting blood gas transfer in patients with acute respiratory failure. *Artif Organs* 16: 75–82, 1992.
4. Conrad SA, Bagley A, Bagley B, *et al.*: Major findings from the clinical trials of the intravascular oxygenator. *Artif Organs* 18: 846–863, 1994.
5. Hattler BG, Reeder GD, Sawzik PJ, *et al.*: Development of an intravenous membrane oxygenator: enhanced intravenous gas exchange through convective mixing of blood around hollow fiber membranes. *Artif Organs* 18: 806–812, 1994.
6. Federspiel WJ, Hewitt T, Hout MS, *et al.*: Recent progress in engineering the Pittsburgh Intravenous Membrane Oxygenator. *ASAIO J* 42: M435–M442, 1996.
7. Ward-Smith AJ: *Internal Fluid Flow: The Fluid Dynamics of Flow in Pipes and Ducts.* Oxford, Clarendon Press, 1980.
8. Macha M, Federspiel WJ, Lund LW, *et al.*: Acute *in-vivo* studies of the Pittsburgh Intravenous Membrane Oxygenator. *ASAIO J* 42: M609–M615, 1996.
9. Vaslef SN, Mockros LF, Anderson RW, Leonard RJ: Use of a mathematical model to predict oxygen transfer rates in hollow fiber membrane oxygenators. *ASAIO J* 40: 990–996, 1994.